Resonant Inelastic X-Ray Scattering in Hexagonal Boron Nitride Observed by Soft-X-Ray Fluorescence Spectroscopy

J. J. Jia and T. A. Callcott
University of Tennessee, Knoxville, Tennessee 37996

Eric L. Shirley
National Institute of Standards and Technology, Gaithersburg, Maryland 20899

J. A. Carlisle, L. J. Terminello, and A. Asfaw
Lawrence Livermore National Laboratory, Livermore, California 94551

D. L. Ederer
Tulane University, New Orleans, Louisiana 70118

F. J. Himpsel
University of Wisconsin-Madison, Madison, Wisconsin 53706

R. C. C. Perera
Lawrence Berkeley Laboratory, Berkeley, California 94720

(Received 3 November 1995)

Photon-excited B *K* fluorescence spectra were measured for hexagonal boron nitride using tunable synchrotron radiation below and above the B *K* edge. We report Raman-like resonant inelastic scattering of soft x rays involving excitation of delocalized valence-band electrons. The inelastic scattering features track with the excitation energy below threshold, go through a resonance as the excitation is tuned to the B(1*s*) core-exciton energy, and evolve into incoherent fluorescence as the excitation is raised further. The energy loss is identified as equivalent to an electronic transition of valence σ electrons to π^* conduction-band states. [S0031-9007(96)00211-6]

PACS numbers: 78.70.Ck, 78.70.En

Interest in inelastic x-ray scattering has been stimulated by the development of high-brightness synchrotron radiation sources. Most of the work has examined the scattering of high-energy (keV) x rays by inner-core electrons, where the systems are left with a localized core hole in the final state [1–3]. However, recent resonant-fluorescence studies, where the systems are left in delocalized *valence-excited* states (i.e., valence-hole final states), have revealed resonant inelastic scattering processes which conserve crystal momentum in Si, diamond, and graphite [4–6]. The theory of coherent fluorescence, as put forward for localized atomic systems by Åberg and Tulkki [7,8], and recently extended to solid-state systems with delocalized electrons by Ma *et al.* [5], predicts this crystal momentum conservation well when the excitation energy is *above* the core-level absorption threshold.

In this Letter, we report the observation of inelastic scattering in hexagonal boron nitride (*h*-BN) for excitation *below* the B *K* edge. We also show that an extension of the theory to below threshold excitation predicts the overall experimental spectra quite well. The disagreement between theory and experiment is attributed chiefly to core-excitonic effects, which are strong in this system and clearly observed. These results demonstrate that the resonant fluorescence technique can yield element-specific band structure information on multielement insulating materials.

Using x-ray fluorescence detection and a large (1 eV) bandpass monochromator, O'Brien *et al.* [9] observed large energy shifts in fluorescence spectra of *h*-BN and B_2O_3 for excitation of B(1*s*) electrons to form core excitons. The excitonic electron, bound in a localized orbital near the core hole, acted as a "spectator" electron which changed the screening and caused an energy shift of the "normal" fluorescence spectrum. Substantial changes in the shape of the *h*-BN spectrum were noted, but not discussed in any detail. In other reports, the large magnitude of the elastic peaks for resonant-fluorescence (spectator) emission from *h*-BN [10] and B_2O_3 [11] have been documented, but little attention was paid to valence-fluorescence (normal) emission.

The soft-x-ray fluorescence (SXF) spectra were obtained using photons from beam line 8.0 at the Advanced Light Source (ALS). Traditionally, SXF spectroscopy has been severely limited by weak excitation sources and low radiative yields of the emission process. However, with the development of intense undulator-based synchtrotron radiation sources and improved spectrometers, many new experiments are now feasible. A crushed-powder sample was used for the experiment. The energy resolution of the monochromatic light used for excitation was set at 0.3 eV.

Emitted radiation was measured with a Rowland-circle-type spectrometer [12] utilizing large spherical gratings and a photon-counting area detector. The spectrometer was operated at a resolution of 0.5 eV for the B *K* edge. Incident photon flux was monitored by measuring photocurrent from a gold-coated screen inserted in the beam immediately upstream from the sample.

Figure 1 shows the SXF spectra of *h*-BN excited with photon energies near the B *K* edge, showing inelastic scattering and valence-band fluorescence. All spectra shown are normalized to the incident photon flux, and labeled by the excitation energy. For display purposes, the elastic peaks are reduced, and the spectra for 192.0 and 192.6 eV excitation are reduced, as indicated. The principal feature of the elastic peak is the very strong resonance observed at 192.0 eV, when B(1*s*) electrons are presumably excited into an exciton state involving the B π^* orbital. The intensity of the elastic peak increases roughly 400-fold as the excitation changes from 186.8 to the resonance at 192.0 eV.

For all excitation energies below 192.0 eV (resonance), the inelastic spectra show two peaks *A* and *B* separated by 5 eV, and the much more intense elastic peak *D*. These spectral features exactly track the excitation energy, so that the upper peak of the inelastic spectrum (peak *B*) maintains a constant separation of $\sim$11 eV from the elastic peak. At resonance excitation (192.0 eV), a new feature appears in the inelastic spectrum, i.e., a shoulder (peak *C*), about 2.5 eV above peak *B*. At higher excitation energies, peak *C* disappears. For 193.7 eV and higher excitation energies, fluorescence features are broadened and become fixed in energy position. These spectra are characteristic of incoherent spectra generated when the excitation and emission processes are decoupled.

A layered structure similar to graphite, *h*-BN [13], has sp^2 σ bonds in planes of atoms and π bonds normal to the plane. The quasiparticle band structure is shown in Fig. 2. The many-body corrections to our density-functional band energies were taken from Blase *et al.* [14]. It displays an indirect band gap of 5.5 eV with the valence band maximum at *H* and conduction band minimum at *M*. The band separation at *M* (6.1 eV) agrees well with optical absorption data [15], which indicates strong intrinsic interband transitions at 6.2 eV. Previous calculations by Catellani, Posternak, and Baldereschi [16] and by Ma *et al.* [17] yielded very similar bands for *h*-BN, but underestimate the band gap significantly.

Figure 3 shows a schematic of the inelastic scattering processes at the B *K* edge. The physics of the scattering is given by the Kramers-Heisenberg formula, which results from the application of time-dependent perturbation theory in second order [18]:

$$\frac{d\sigma}{d\Omega} \propto \sum_f \left| \sum_m \frac{\langle f|pA|m\rangle\langle m|pA|i\rangle}{E_m - E_i - h\nu_{\text{in}} - i\Gamma_m/2} \right|^2 \times \delta(E_f + h\nu_{\text{out}} - E_i - h\nu_{\text{in}}) . \tag{1}$$

In this expression, $|i\rangle$ is the initial (ground state) of the system with energy E_i, $|m\rangle$ is one of an ensemble of intermediate states to be summed over, which have a core hole in the B(1*s*) core level and an electron in a

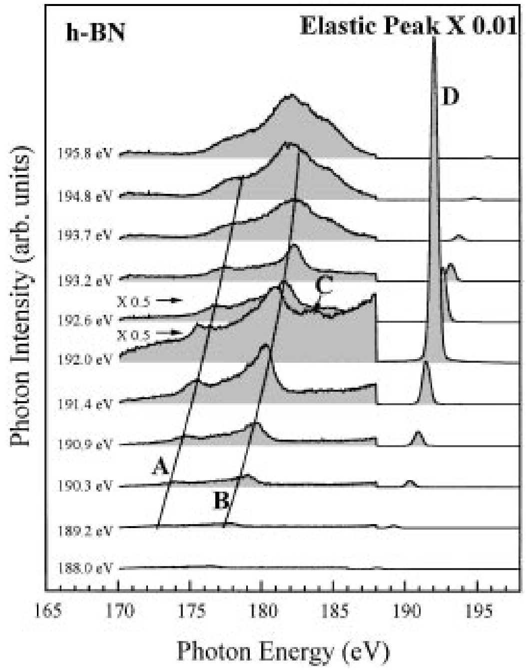

FIG. 1. The B *K*-edge soft-x-ray fluorescence spectra of *h*-BN for excitation near threshold. Labeled features are discussed in the text. The elastic peaks of all spectra are reduced as indicated, and the valence spectra excited by 192.0 and 192.6 eV photons are reduced as indicated.

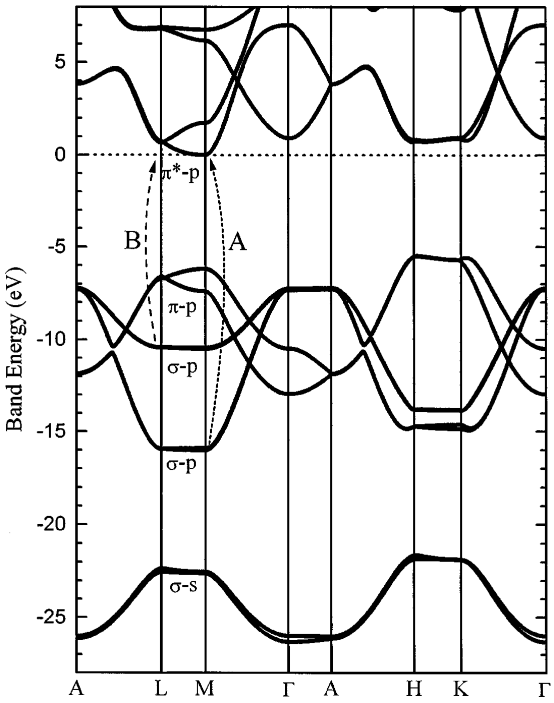

FIG. 2. The *h*-BN quasiparticle band structure. Transitions proposed for peaks *A* and *B* (cf. Fig. 1) are indicated.

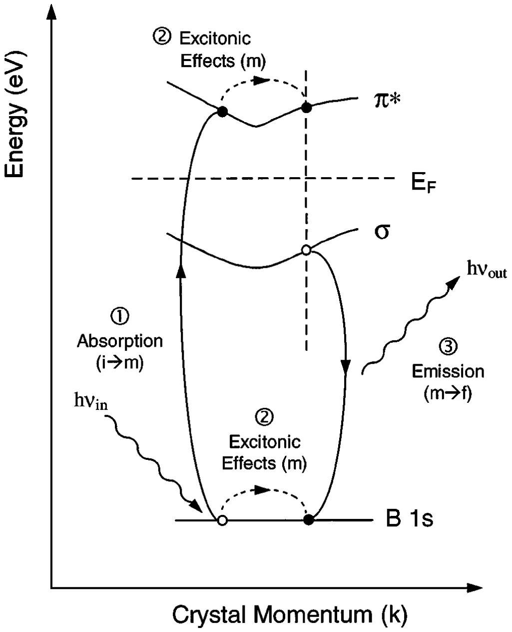

FIG. 3. Illustration of the absorption-emission process using a "three step" picture. Steps are (1) absorption, (2) core-hole excitonic effects, causing core hole and promoted electron to migrate together in Brillouin zone, and (3) emission. States or transitions between states associated with these steps and Fermi level indicated. The notion of "steps" is used only for illustration and conceptual purposes.

conduction-band state, and $|f\rangle$ is the final state, which consists of an electron in a conduction band state and a hole in a valence-band state (Fig. 3). The energy-conserving delta function requires that the energies of the incident and emitted photons be related to the energies of the electron and hole by

$$h\nu_{\text{in}} - h\nu_{\text{out}} \cong E_e(\mathbf{k}_e) - E_h(\mathbf{k}_h)\,. \tag{2}$$

If the appropriate wave functions (Bloch functions) are substituted into the Kramers-Heisenburg formula above, a crystal-momentum conservation rule follows, involving momenta of photons, electron, and hole [5]:

$$q_{\text{in}} - q_{\text{out}} = \mathbf{k}_e - \mathbf{k}_h + \mathbf{G}\,. \tag{3}$$

While fluorescence may be described by Eq. (1) for both above and below threshold excitation, below-threshold scattering involving delocalized intermediate and final states has not been reported. In the more familiar case, i.e., above-threshold excitation, the energy denominator in Eq. (1) resonantly enhances intermediate states which have energies satisfying the condition $E_m \cong E_i + h\nu_{\text{in}}$. Energy is approximately conserved in the virtual transition of the core electron to the conduction band. This energy selectivity in the intermediate state allows Eq. (2) to be decoupled into two equations, leading in general to crystal-momentum selectivity for final electron and hole momenta, and the mapping of band structure [6]. Incoherent processes (i.e., the normal two-step absorption followed by emission process) also compete with the coherent fluorescence process in the above-threshold excitation regime, so that spectra obtained above threshold have a finite incoherent fraction ($>10\%$), which increases rapidly with the excitation energy.

For excitation below the core threshold, the scattering should be very different. Firstly, the scattering must be purely coherent. Note that no trace of the normal B K valence emission is present for $h\nu_{\text{in}} \leq 192$ eV. Secondly, the energy denominators in Eq. (1) possess no minima for below threshold excitations. This is simply due to the minimum energy needed to create a core-hole state $|m\rangle$, i.e., the B(1s) binding energy (or core exciton binding energy, see below). Crystal momentum is still conserved, but no selectivity takes place as it does for above threshold excitation. Equation (2) cannot be decoupled in the manner described above, so that the allowed emission energies are obtained by simply solving Eq. (2) for $h\nu_{\text{out}}$:

$$h\nu_{\text{out}} = h\nu_{\text{in}} - [E_e(\mathbf{k}_e) - E_h(\mathbf{k}_h)]\,. \tag{4}$$

Consequently, for a given final state $h\nu_{\text{out}}$ will track $h\nu_{\text{in}}$ linearly, and the magnitude of the energy loss is constant (independent of $h\nu_{\text{in}}$) and equivalent to an interband transition energy. It is a soft-x-ray form of Raman scattering. Since crystal momentum is still conserved, the magnitude of the energy loss is the partial joint density of states (p-JDOS).

With the quasiparticle band structure and Eq. (1), we have simulated fluorescence spectra in an independent, quasiparticle model, using a detailed description of quasiparticle wave functions and energies. The Born-Heisenberg formula was used, and the matrix elements between initial, intermediate, and final states were approximated as one-electron matrix elements. The energies of the excited states were based on quasiparticle energies. We have not included excitonic or other complicating effects in this model, but their inclusion at the same level of detail as the quasiparticle description of electrons would be profitable.

The calculated, purely coherent fluorescence spectra are shown in Fig. 4, as well as an incoherent spectrum, which is a summation of the recombination matrix-element-weighted density of states. Within our simple model, there is general agreement between experimental and calculated spectra regarding energy position, energy dispersion, and intensity variation of peaks A and B. The simulations indicate a dominance of B(1s) $\rightarrow \pi^*$ and $\sigma \rightarrow$ B(1s) channels in the absorption and emission processes, respectively. Transitions associated with peaks A and B correspond well with σ (valence) $\rightarrow \pi^*$ (conduction) separations near M in the band structure shown in Fig. 2. Experimentally, these features are greatly enhanced compared to the independent quasiparticle picture, presumably because of excitonic effects. Feature C, which appears at an excitation energy of 192.0 eV, is not detected in the simulations. It may result purely from excitonic or other mechanisms.

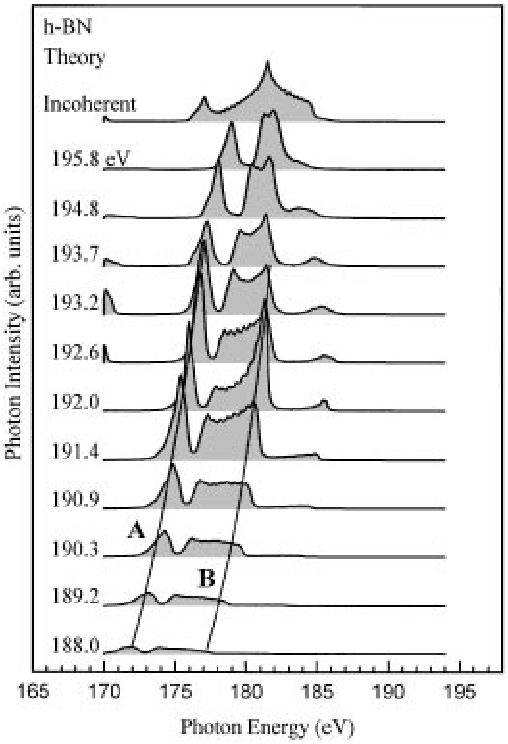

FIG. 4. Simulated fluorescence spectra for *h*-BN for different excitation energies, plus incoherent spectrum. Quasielastic features were not included in the theory.

There are also obvious differences between the theory and experiment, probably because of neglect of excitonic effects in our theory. The π^* states at the conduction band minimum should dominate the intermediate states near threshold, but interactions between the core hole and the excited electron have yet to be incorporated into the theory. The resemblance of the spectra above threshold to the calculated incoherent spectrum indicates that incoherent processes dominate coherent ones when the core electron is excited above the conduction band minimum. The calculated incoherent spectrum has very sharp peaks, indicating broadening mechanisms which are not included in the theory, since the instrumental resolution is only 0.5 eV. Earlier work on *h*-BN suggests phonon broadening effects may play an important role in core-level spectra [19]. Enhancement of the incoherent signal is a possible by-product of such mechanisms.

To summarize, we have reported the observation of Raman-like loss features in *h*-BN fluorescence measurements for excitation energies below the B *K* edge. We have shown that a simple extension of the theory of coherent fluorescence to below-threshold excitation, based on the quasiparticle band structure, accounts for much of the experimental data. The disagreement between theory and experiment is thought to arise from excitonic effects in the resonant scattering process. We are currently working to extend the theory to include excitonic effects.

This research was partially supported by NSF Grants No. DMR-9017996 and No. DMR-9017997, by the Science Alliance Tennessee Center of Excellence at the University of Tennessee, by DOE Contract No. W-7405-ENG-48 at Lawrence Livermore National Laboratory, and by the Louisiana Educational Quality Support Fund and DOE-EPSCOR Grant No. LEQSF (93-95)-03 at Tulane University. The experiment was performed at the Advanced Light Source at Lawrence Berkeley National Laboratory, which is supported by DOE Contract No. DE-AC03-76SF00098.

[1] C. J. Sparks, Phys. Rev. Lett. **33**, 262 (1974).

[2] P. Eisenberger, P. M. Platzman, and H. Winick, Phys. Rev. Lett. **36**, 623 (1976).

[3] J. P. Briand, D. Girard, V. O. Kostroun, P. Chevalier, K. Wohrer, and J. P. Mosse, Phys. Rev. Lett. **46**, 1625 (1981).

[4] J-E. Rubensson, D. R. Mueller, R. Shuker, D. L. Ederer, C. H. Zhang, J. J. Jia, and T. A. Callcott, Phys. Rev. Lett. **64**, 1047 (1990); K. E. Miyano, D. L. Ederer, T. A. Callcott, W. L. O'Brien, J. J. Jia, L. Zhou, Q.-Y. Dong, Y. Ma, J. C. Woicik, and D. R. Mueller, Phys. Rev. B **48**, 1918 (1993).

[5] Y. Ma, N. Wassadahl, P. Skytt, J. Guo, J. Nordgren, P. D. Johnson, J. E. Rubensson, T. Boske, W. Eberhardt, and S. D. Kevan, Phys. Rev. Lett. **69**, 2598 (1992); Y. Ma, Phys. Rev. B **49**, 5799 (1994).

[6] J. A. Carlisle, E. L. Shirley, E. A. Hudson, L. J. Terminello, T. A. Callcott, J. J. Jia, D. L. Ederer, R. C. C. Perera, and F. J. Himpsel, Phys. Rev. Lett. **74**, 1234 (1995).

[7] T. Åberg and J. Tulkki, in *Atomic Inner-shell Physics*, edited by B. Crasemann (Plenum, New York, 1985), Chap. 10, pp. 419–463, and references therein.

[8] J. Tulkki and T. Åberg, J. Phys. B **15**, L435 (1982); J. Tulkki, Phys. Rev. A **27**, 3375 (1983).

[9] W. L. O'Brien, J. J. Jia, Q.-Y. Dong, T. A. Callcott, K. E. Miyano, D. L. Ederer, D. R. Mueller, and C.-C. Kao, Phys. Rev. Lett. **70**, 238 (1993).

[10] J. A. Carlisle, R. C. C. Perera, J. H. Underwood, L. J. Terminello, E. A. Hudson, T. A. Callcott, J. J. Jia, and F. J. Himpsel, Appl. Phys. Lett. **67**, 34 (1995).

[11] Y. Muramatsu, M. Oshima, and H. Kato, Phys. Rev. Lett. **71**, 448 (1993).

[12] J. J. Jia, T. A. Callcott, J. Yurkas, A. W. Ellis, F. J. Himpsel, M. G. Samant, J. Stohr, D. L. Ederer, J. A. Carlisle, E. A. Hudson, L. J. Terminello, D. K. Shuh, and R. C. C. Perera, Rev. Sci. Instrum. **66**, 1394 (1995).

[13] R. S. Pease, Acta. Crystallogr. **5**, 356 (1952).

[14] X. Blase, A. Rubio, S. G. Louie, and M. L. Cohen, Phys. Rev. B **51**, 6868 (1995).

[15] A. Zunger, A. Katzir, and A. Halperin, Phys. Rev. B **13**, 5560 (1976).

[16] A. Catellani, M. Posternak, and A. Baldereschi, Phys. Rev. B **36**, 6105 (1987).

[17] H. Ma, S. H. Lin, R. W. Carpenter, P. Rice, and O. F. Sankey, J. Appl. Phys. **73**, 7422 (1993).

[18] See, for example, J. J. Sakurai, *Advanced Quantum Mechanics* (Addison-Wesley, Reading, Massachusetts, 1967), Chap. 2.

[19] A. Mansour and S. E. Schnatterly, Phys. Rev. Lett. **59**, 567 (1987).